ATMOSPHERIC SCIENCE LETTERS
Atmos. Sci. Let. **11**: 180–185 (2010)
Published online 10 March 2010 in Wiley Online Library
(wileyonlinelibrary.com) **DOI:** 10.1002/asl.265

RMetS
Royal Meteorological Society

Low-frequency climate variability in the Atlantic basin during the 20th century

Y. M. Tourre,[1,2] S. Paz,[3]* Y. Kushnir[2] and W. B. White[4]
[1]*METEO-France, Toulouse, France*
[2]*LDEO of Columbia University, Palisades, NY, USA*
[3]*Department of Geography and Environmental Studies, University of Haifa, Haifa, Israel*
[4]*Scripps Institution of Oceanography, University of California, San Diego, La Jolla, CA, USA*

*Correspondence to:
S. Paz, Department of Geography and Environmental Studies, University of Haifa, Abba Hushi road, Mt. Carmel, Haifa, Israel.
E-mail: shlomit@geo.haifa.ac.il

Received: 20 May 2009
Revised: 17 January 2010
Accepted: 2 February 2010

Abstract

From joint sea surface temperature/sea level pressure (SST/SLP) EOF analyses, low-frequency variability modes are compared. The multi-decadal oscillation (MDO) changed phases twice during the 20th century, with its north Atlantic SST patterns resembling the Atlantic multi-decadal oscillation (AMO). The quasi-decadal oscillation (QDO) SST patterns displayed a double tripole configuration over the entire Atlantic basin, leading to tropical inter-hemispheric out-of-phase relationship. From the mid-1960s onward, while SST anomalies were negative to the north (negative phases of MDO/AMO), the Sahelian drought persisted with a weaker hurricane power dissipation index (PDI). During that period, the QDO modulated the intensity of the Sahelian drought. Copyright © 2010 Royal Meteorological Society

Keywords: multi-decadal oscillation; quasi-decadal oscillation; Sahelian drought; power dissipation index

1. Introduction

Low-frequency global climate signals include the global multi-decadal oscillation (MDO; Schlesinger and Ramankutty, 1994) and the global quasi-decadal oscillation (QDO; Mann and Park, 1994). SST multi-decadal variability in the Atlantic Ocean is referred to as the Atlantic multi-decadal oscillation/variability (AMO; Kerr, 2000). The AMO is linked to the thermohaline circulation (THC; Zhang, 2007). Thus when depth integrated Atlantic flow anomalies have been reconstructed, minimum values in the mid-to-late 1960s equivalent to −1.2 Sv (present-day levels are ∼0.63 Sv) were identified when the AMO changed its phase (Knight *et al*., 2005). Multi-decadal signals have also been detected in proxy records, such as Caribbean coral data (Hetzinger *et al*., 2008).

Linkages exist between global low-frequency climate oscillations in the eastern Mediterranean, eastern USA and Eurasian climates (Enfield *et al*., 2001; D'Aleo, 2007; Paz *et al*., 2008), Sahelian rainfall (Zhang and Delworth, 2006), and Atlantic hurricanes (Vimont and Kossin, 2007). Based on previous results and in the light of new results presented here during the 20th century, mechanisms and variability for MDO and QDO are further discussed and compared with other indices. This research is to contribute to a better understanding of the evolution of two distinct low-frequency climate signals in the Atlantic. Following Keenlyside *et al*. (2008) forced anthropogenic climate change is to interfere with such low-frequency natural and internal climate variability, expected to bring socio-economical burden.

2. Data and methods

Tourre and White (2006) analyzed global climate signals during the 20th century, SST/SLP datasets being submitted to the MTM/SVD technique (Mann and Park, 1999). Significant frequency bands were identified. Here SLP and SST-gridded fields from the GMSLP/GISST datasets (Basnett and Parker, 1997; Rayner *et al*., 2003) are submitted to low-passed (40-year) and band-passed (8–14 years) recursive filter (Kaylor, 1977), prior to further EOF analysis.

To reconcile results from the literature, seasonal lead/lag correlations (significant at the 0.05 level using p-values from the Z-test) between different indices are also computed and compiled in Table I. Statistical significance takes into account the effects of serial correlations following Dawdy and Matalas (1964). The time-series/indices used are:

(1) SST in the tropical north Atlantic (TNA), SST in the tropical south Atlantic (TSA), and TNA−TSA derived from Rajagopalan *et al*. (1998).
(2) Rotated EOF amplitude function of the Sahelian rainfall mode, adapted from Rogel *et al*. (2006).
(3) Derived Power Dissipation Index (PDI; courtesy of Kerry Emanuel). The PDI is the time integral of the cube of maximum sustained wind speed at ∼10 m. Corrected wind dataset is available at:

Table I. Significant seasonal correlations between known Atlantic indices and climate time-series are discussed throughout the article.

Time-series and indices	Seasons	*r*-Values
AMM (SST) and AMO	Summer	0.72
AMM (Wind) and AMO	Spring	0.63
AMM (SST) and AMM (Wind)	Summer	0.70
AMM (SST) and TNA	Fall	0.68
	Winter	0.73
	Spring	0.84
	Summer	0.76
AMM (SST) and TNA−TSA	Spring	0.80
	Summer	0.72
AMM (Wind) and TNA−TSA	Spring	0.68
	Summer	0.47
AMM (Wind) and Sahelian rainfall	Summer	0.65
AMM (SST) and Sahelian rainfall	Summer	0.42
TNA−TSA and Sahelian rainfall	Summer	0.36
TNA−TSA and Sahelian rainfall	Fall	0.40
AMM (Wind) and mean # of hurricanes	Summer	0.47
AMM (SST) and mean # of hurricanes	Summer	0.45
AMM (SST) and mean # of hurricanes	Fall	0.55
AMM (Wind) and hurricane mean wind-speed	Summer	0.51
AMM (SST) and hurricane mean lowest pressure	Spring	−0.49
AMM (SST) and hurricane mean lowest pressure	Summer	−0.49
TNA−TSA and maximum hurricane types	Fall	0.40
AMM (SST) and PDI	Summer	0.61
AMM (Wind) and PDI		0.58
AMM (SST) and PDI	Fall	0.66
AMM (Wind) and PDI		0.51

All maximum seasonal correlations with no lags (seasonal lags are implicit) are significant with at least 0.05% confidence estimated from *p*-values of *Z*-test method that takes into account serial correlations.

http://www.aoml.noaa.gov/hrd/hurdat/metadata_JUL08.html/.

(4) Sahelian rainfall index from the JISAO site at University of Washington: http://jisao.washington.edu/data/sahel/).

(5) The Atlantic Meridional Mode or AMM (SST and Wind) indices from CDC/NOAA: http://www.cdc.noaa.gov/Timeseries/Monthly/AMM.
Data is from the University of Wisconsin using NCEP SST data.

(6) Yearly Atlantic Tropical Cyclones or ATC (June–October) parameters, i.e. numbers, lowest pressure, wind speed (km/h) and hurricane types from the HURDAT dataset at NOAA/Hurricane Research Division site: http://www.aoml.noaa.gov:80/hrd/hurdat/tracks1851to2006_atl.txt.
See also Jarvinen *et al*. (1984).

3. Results

The 40-year low-passed MDO joint SLP/SST spatio-temporal climate patterns from the EOF analysis are displayed in Figure 1. Little changes in patterns occurred when 30-year and 50-year low-passed filters were applied. The MDO SLP patterns are stronger in the Pacific and Atlantic oceans. Nevertheless from the Indian to the Atlantic oceans, SLP negative/positive anomalies display maximum/minimum variability in the tropical belt only. Tropical alternated polarities could reflect variability in ascendance/subsidence from tropospheric zonal cells (Figure 1, bottom left). The Southern Oscillation Index (SOI) is thus modulated by the global MDO, corroborating results from proxy records (Cook *et al*., 2008).

The MDO SST patterns have similar intensity in the three oceans, with Atlantic SST 'signature' resembling anomaly patterns in Delworth and Mann (2000), i.e. the AMO. Reversed polarity is found between the northern/tropical Atlantic until 10 °S and the southern Atlantic. Extrema of SST anomalies in the northern part are around 1910 (minimum), 1950 (maximum) and 1990 (minimum). Phase changes of the MDO are conspicuous in the mid-1920s and late 1960s and early 1970s, when the AMO also changed phases. In-phase SST anomalies relationship are found between the Indian Ocean, the central equatorial Pacific Ocean, and the southern Atlantic Ocean (Figure 1, bottom right).

The 8–14 years band-passed Atlantic QDO joint SLP/SST spatio-temporal climate patterns from the EOF analysis are displayed in Figure 2. The QDO has been identified as a global signal but its 'signature' is confined to the tropics in the Pacific (Tourre *et al*., 2001). This is quite different to its global Atlantic meridional 'signature' where double SST tripole spatial patterns are well structured in the northern Atlantic and the southern Atlantic, leading to a low-frequency out-of-phase SST relationship in the tropical Atlantic (i.e. quasi-decadal). SLP anomalies also display opposite polarity between the northern and the southern Atlantic regions. SST/SLP patterns are relatively weaker during the 1900–1915, 1950–1960 and 1990–2000 periods. The joint SST/SLP patterns are indicative of a quasi-decadal out-of-phase oscillation in the strengths of the subtropical anticyclones (i.e. of trade-winds and ITCZ location). These joint spatial patterns were best established between the mid-1960s until the late 1980s alternating with MDO minima during the late 1930s and early 1970s (Figure 2, top).

The MDO amplitude function is super-imposed on the tropical SST anomaly differences or TNA−TSA (Figure 3, top). TNA−TSA is mostly negative until the mid-1920s (MDO and AMO cold phases in the north Atlantic), positive from the mid-1920s until late 1960s (MDO and AMO warm phases in the north Atlantic), and negative from the late 1960s onward (during MDO and AMO cold phases until the mid-1990s in the north Atlantic). A smoothed normalized PDI is also super-imposed in Figure 3 (red, top). Overall negative values of the index are clearly seen during the negative phases of the MDO and AMO in the northern Atlantic. Positive values of the PDI are found after 1995, when the AMO index indeed changed phase (Enfield *et al*., 2001).

The TNA−TSA index matches quite well the band-passed QDO amplitude function, as seen in Figure 3

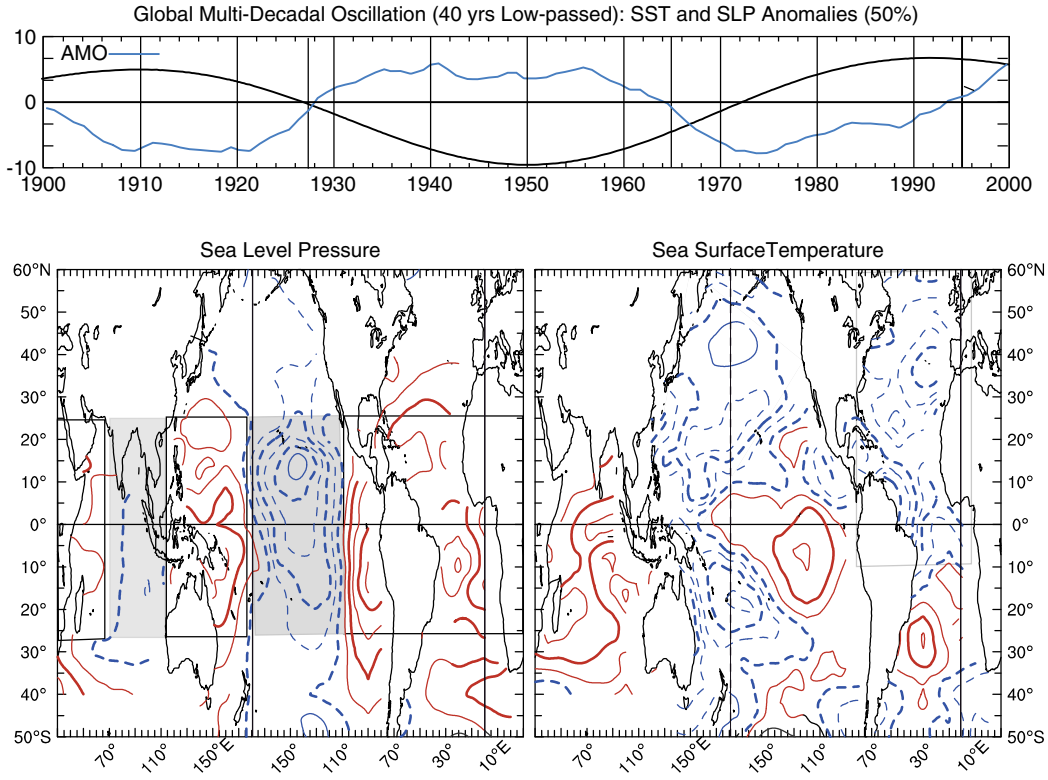

Figure 1. Global MDO from joint SST/SLP EOF analysis of 40-year low-passed time-series representing 50% of the variance of the low-passed data. Normalized amplitude function (top), SLP (bottom left) and SST (bottom right) maximum loadings are displayed. Isolines every 0.05 hPa (SLP) and 0.05 °C (SST) correspond to maxima of 0.25 hPa and ~0.15 °C. Red/dashed-blue isolines are for positive/negative values. Tropical rectangles are to highlight alternating tropical SLP patterns (bottom left). A smoothed (121-month smoother) AMO (detrended, area-weighted average from 0° until 70 °N) is superimposed.

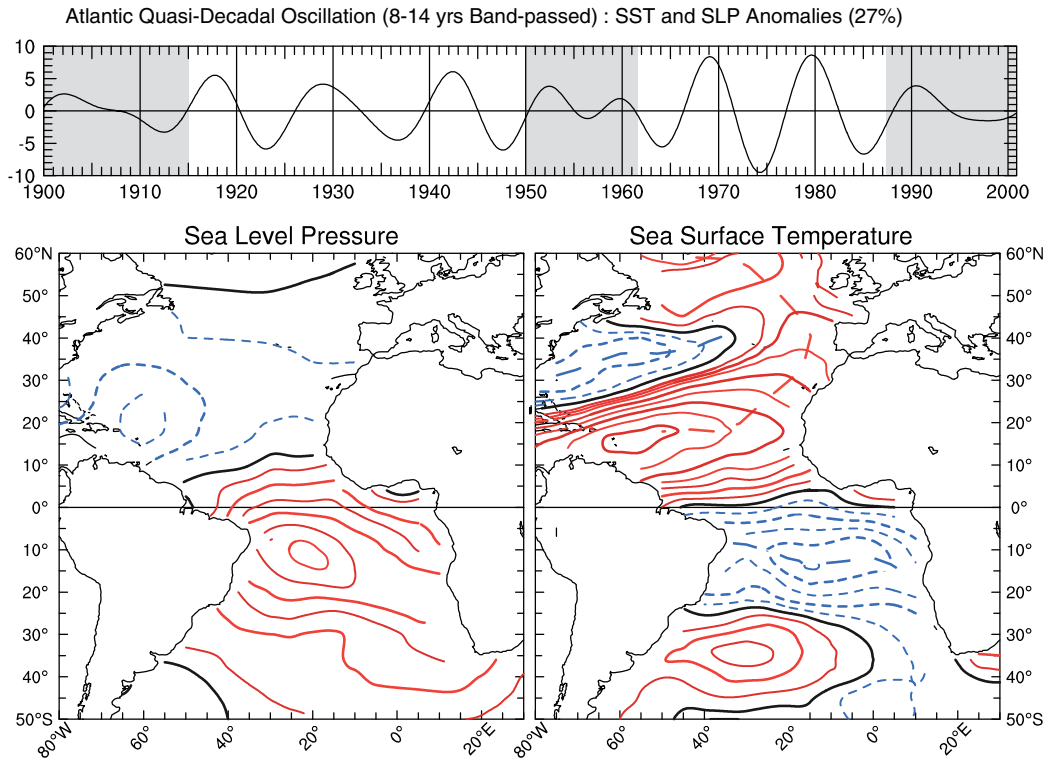

Figure 2. Atlantic QDO from joint SST/SLP EOF analysis. The signal has been 8–14 years band-passed and represents 27% of the band-passed variance. Normalized amplitude function (top), SLP (bottom left) and SST (bottom right) maximum loadings are displayed. Isolines are every 0.05 hPa (SLP) and 0.05 °C (SST) thus corresponding to maxima of 0.30 hPa and of 0.35 °C. Red/dashed-blue isolines are for positive/negative values. The thick black lines are for zero values. Gray shading (top) highlights periods with weak QDO climate signal.

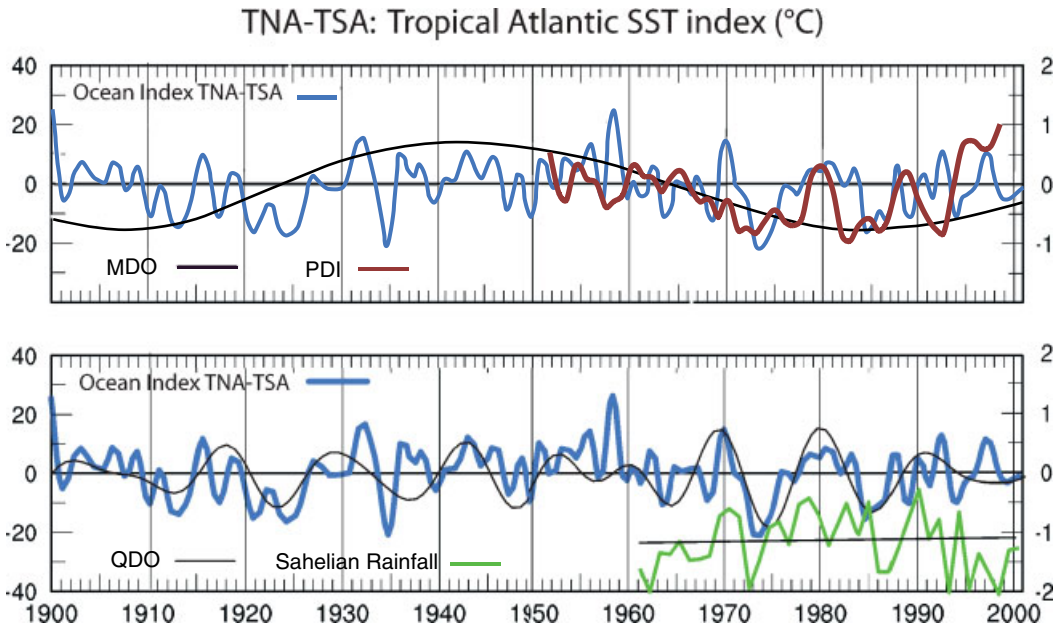

Figure 3. Top: From TNA (5 °N to 20 °N; and 20 °W to 40 °W) and TSA (5 °S to 15 °S; 15 °W to 5 °E), TNA−TSA (thick solid blue line) anomalies are displayed. Units are in °C (right ordinates). The Atlantic MDO (thin black line) with reversed amplitude function is displayed. Standard deviation × 10 (left ordinates). Vertical lines in the mid-1920s, late 1960s are for MDO phase changes. Bottom: The TNA−TSA (in °C, right ordinates) time-series is displayed (solid blue line) along with the QDO (thin black line) amplitude function from Figure 2 (top). Standard deviation × 10 (left ordinates). A smoothed (3-year averaging) and normalized PDI index is shown (red line, top). The amplitude function of the rotated EOF second mode (green line, bottom right) of West African rainfall data representing Sahelian rainfall is displayed (11.9% of total variance). The zero-line of the normalized Sahelian rainfall mode is displaced for easy comparison.

(bottom). The TNA−TSA variability is linked to the ITCZ location over the eastern Atlantic and West Africa (Giannini *et al*., 2003). The amplitude function of the Sahelian rainfall rotated empirical orthogonal function mode (11.9% of total variance) is reproduced in Figure 3 (green, staggered zero-line, bottom right). Sahelian rainfall anomalies are less negative in the early 1970s, 1980s and 1990s, e.g. during MDO and AMO negative phases, and period of the long-lasting Sahelian drought. Thus the MDO/AMO and QDO can be perceived as independent climate signals whose variability modulate Sahelian rainfall and drought intensity.

To better compare the above results with others, significant correlations, i.e. maximum seasonal lead/lag values at the 0.05 level (Z-test), between AMM (SST and Wind), TNA, TNA−TSA, Sahelian rainfall, hurricanes parameters and PDI, are computed and presented in Table I. Correlations between AMO (from Enfield *et al*., 2001) and AMM (SST and Wind) time-series are given for completeness.

3.1. Comparing AMM (SST and Wind) with TNA, TNA−TSA (QDO climate proxy) time-series

It has been shown that the AMO has maximum loadings in the northern Atlantic (Mestas-Nuñez and Enfield, 1999) reflecting high correlation between the AMO summer SST anomalies and AMM SST and Wind ($r = 0.72$; 0.63 respectively). Moreover, TNA and TNA−TSA time-series are quite similar. This explains why here high seasonal correlations exist between AMM (SST) and TNA, and AMM (SST and Wind) and TNA−TSA (Table I). Mostly negative values for the four indices are found from the mid-1960s until the mid-1990s (not shown). This further corroborates the relationships between QDO and tropical AMM (SST and Wind) variability.

The following two sections 3.2. and 3.3. are to integrate results from previous research in the context of the low-frequency natural climate variability discussed here.

3.2. Comparing AMM (SST and Wind) time-series with Sahelian rainfall index

The low-frequency variability of Sahelian rainfall has been mentioned in several works. Here high seasonal correlations are also found between AMM (SST and Wind), TNA−TSA and Sahelian rainfall (Table I). Mostly negative values of summer AMM (Wind) and Sahelian rainfall index are found from late 1960s until late 1990s, the period of the last Sahelian drought.

3.3. Comparing AMM (SST and Wind), ATC parameters time-series and PDI index

High seasonal correlations between AMM (SST and Wind) variability and ATC parameters (mean number of hurricanes, hurricane mean wind-speed, lowest pressures and types) are comparable with that from Vimont and Kossin (2007). High correlations are found between summer/fall AMM (SST and Wind) time-series and the PDI index. Minimum values during

summer/fall AMM (SST and Wind) time-series and PDI, are found from late 1960s until mid-1990s period (not shown) when the overall number of major hurricanes is also below average (Goldenberg *et al*., 2001). The correlation between fall TNA−TSA and hurricanes type is of $r = 0.40$. As already mentioned, overall PDI negative values since the late 1960s (besides 1978−1982 when the QDO was peaking) are conspicuous (Figure 3, top).

4. Discussion and conclusion

From a new joint SST/SLP EOF analysis, spatio-temporal evolutions of two lead low-frequency climate signals over the Atlantic basin, i.e. the MDO or AMO (if only SST variability is considered) and the QDO are investigated during the 20th century. Distinctive SST/SLP spatial patterns for MDO and QDO climate signals correspond to different physical mechanisms. The MDO climate signal could include a stochastic excitation by the global atmosphere of an Atlantic internal mode, propagation of heat content (subduction) and temperature anomalies from mean currents and interaction with the overlying atmosphere (Delworth and Mann, 2000; Dijkstra *et al*., 2006). Resulting SST patterns may modify the overlying atmosphere and the standing NAO index (see also Mestas-Nuñez and Enfield, 1999). The MDO SLP patterns are mainly tropical (i.e. distinct from the Pacific decadal oscillation) and associated with SOI low-frequency variability, linking the tropical Pacific and Atlantic oceans.

QDO variability and joint distribution of SST/SLP patterns indicate faster air−sea interactions, heat flux exchanges and hydrostatic adjustment (Delworth and Greatbatch, 2000), and include tropical AMM SST variability. The QDO displays SST tripole structures distributed in the entire Atlantic. This is different in the Pacific and Indian oceans where tropical and zonal SST/SLP patterns have been associated with delayed action oscillator mechanisms (Tourre *et al*., 2001; White and Tourre, 2007). In the northern Atlantic between the equator and 50 °N, positive/negative SST anomalies are found when weaker/stronger westerlies and trade-winds occur, with a well defined horse-shoe pattern around the anticyclonic gyre. A non-stationary SST dipole structure occasionally occurs in the tropical Atlantic where meridional SST gradients are more typical (Enfield *et al*., 1999).

MDO/AMO and QDO SST/SLP coherent peak patterns reached after spatio-temporal evolution are linked to the intensity and position of the subtropical anticyclones and resulting location of the ITCZ. Therefore, both MDO/AMO and the QDO are tightly linked with low-frequency Sahelian rainfall variability. Variability of SST anomalies in the north Atlantic may enhance/reduce the evolution of West African easterly waves into tropical depressions, necessary conditions for hurricane genesis.

It is acknowledged that the natural MDO/AMO and QDO climate signals could be modified by anthropogenic forcing (Mann and Emanuel, 2006). The AMO which changed phase in the mid-1990s (i.e. back to a warm phase) is expected to exhibit a predominantly positive phase for the upcoming decades (Liles, 2004) which could contribute to the enhancement of Sahelian rainfall. The recent positive phase seems so far weaker to that during the mid-1950s with anomalies smaller than those attributed to anthropogenic climate change (Trenberth and Shea, 2006).

Should a higher level of hurricane destructiveness (Emanuel, 2005) during the upcoming decade be expected with persistent MDO/AMO positive phases, when decadal SST variability within a narrow 10 °N to 20 °N Atlantic belt seems to have entered negative phases (Molinari and Mestas-Nuñez, 2003), along with positive trend in tropospheric shear over the tropical north Atlantic (Vecchi and Soden, 2007)? Could the recent AMO phase change possibly work against a drier Sahel as predicted by Held *et al*. (2005)? These are still open questions requiring more investigation.

Acknowledgements

The authors would like to thank 'Ted' Walker for data processing at SIO of UCSD. Tourre and Kushnir would also like to thank Drs Philippe Dandin, Mike Purdy and Arnold Gordon, Directors of Dclim/Meteo-France, LDEO of Columbia University, and Head of Observational Physical Oceanography at LDEO, respectively. This is an LDEO contribution #7327.

References

Basnett TA, Parker DE. 1997. *Development of the Global Mean Sea Level Pressure Data Set GMSLP2*. Hadley Centre of the UK Met Office. Climate Research Tech, Note 79. Available from the Hadley Centre for Climate Prediction and Research, Meteorological Office, London Road, Bracknell, RS12 2SY, UK.

Cook ER, D'Arrigo RD, Anchukaitis KJ. 2008. ENSO reconstructions from long tree-ring chronologies: unifying the differences? P*resented at the Special Workshop on 'Reconciling ENSO Chronologies for the Past 500 Years'*, Moorea, French Polynesia, 2–3 April 2008.

D'Aleo JS. 2007. The Atlantic multidecadal oscillation (AMO) and winter snowfall in the eastern US and Eurasia. *19th AMS Conference on Climate Variability and Change*, Antonio, Texas. http://ams.confex.com/ams/87ANNUAL/techprogram/paper_11569.

Dawdy DR, Matalas NC. 1964. Statistical and probability analysis of hydrologic data, part III: analysis of variance, covariance and time series. In *Handbook of Applied Hydrology, a Compendium of Water-Resources Technology*, Chow VT (ed). McGraw-Hill Book Company: New York; 8.68–8.90.

Delworth TL, Greatbatch RJ. 2000. Multidecadal thermohaline circulation variability driven by atmospheric surface flux forcing. *Journal of Climate* **13**: 1481–1495.

Delworth TL, Mann ME. 2000. Observed and simulated multi-decadal variability in the Northern Hemisphere. *Climate Dynamics* **16**: 661–676.

Dijkstra HA, Te Raa L, Schmeits M, Gerrits J. 2006. On the physics of the Atlantic multidecadal oscillation. *Ocean Dynamics* **56**: 36–50.

Emanuel K. 2005. Increasing destructiveness of tropical cyclones over the past 30 years. *Nature* **436**: 686–688.

Enfield DB, Mestas-Nuñez AM, Mayer DA, Cid-Serrano L. 1999. How ubiquitous is the dipole relationship in tropical Atlantic

sea surface temperatures. *Journal of Geophysical Research* **104**: 7841–7848.

Enfield D, Mesta-Nuñez AM, Trimble P. 2001. The Atlantic multidecadal oscillation and its relation to rainfall and riverflows in the continental US. *Geophysical Research Letters* **28**: 2077–2080.

Giannini A, Saravanan R, Chang P. 2003. Oceanic forcing of Sahel rainfall on interannual to interdecadal time scales. *Science* **302**: 1027–1030.

Goldenberg SB, Landsea CW, Mesta-Nuñez AM, Gray WM. 2001. The recent increase in Atlantic hurricane activity: causes and implication. *Science* **293**: 474–479.

Held IM, Delworth TL, LU J, Findell KL, Knutson TR. 2005. Simulation of Sahel drought in the 20th and 21st centuries. *Proceedings of the National Academy of Sciences* **102**: 17891–17896.

Hetzinger S, Pfeiffer M, Dullo W-C, Keenlyside N, Latif M, Zinke J. 2008. Caribbean coral tracks Atlantic Multidecadal Oscillation and past hurricane activity. *Geology* **36**: 11–14.

Jarvinen BR, Neumann CJ, Davis MAS. 1984. *A Tropical Cyclone Data Tape for the North Atlantic Basin, 1886–1983: Contents, Limitations, and Uses*. NOAA Technical Memorandum, NWS NHC 22.

Kaylor RE. 1977. Filtering and decimation of digital time series. Tech. Rep. Note, BN850 University of Maryland: College Park, MD.

Keenlyside NS, Latif M, Jungclaus J, Kornblueh L, Roeckner E. 2008. Advancing decadal scale climate prediction in the North Atlantic sector. *Nature* **453**: 43–45. DOI: 10.1038/453043a.

Kerr, RA. 2000. A North Atlantic climate pacemaker for the centuries. *Science* **288**: 1984–1986.

Knight J, Allan RJ, Folland CK, Vellinga M, Mann ME. 2005. A signature of persistent natural thermohaline circulation cycles in observed climate. *Geophysical Research Letters* **32**: L20708. DOI: 10.1029/2005GL024233.

Liles CA. 2004. *Relationships between New Mexico precipitation, the Atlantic Multi-decadal Oscillation and Pacific Decadal Oscillation*. National Weather Service Albuquerque. Available: www.srh.noaa.gov/abq/feature/PDO_and_AMO_and_precip_in_New_Mexico.pdf.

Mann ME, Park J. 1994. Global-scale modes of surface temperature variability on interannual to century timescales. *Journal of Geophysical Research* **99**: 25819–25833.

Mann ME, Park J. 1999. Oscillatory spatio-temporal signal detection in climate studies: a multiple-taper spectral domain approach. *Advances in Geophysics* **41**: 1–131.

Mann ME, Emanuel KA. 2006. Atlantic hurricane trends linked to climate change. *EOS Transactions, AGU* **87**: 233–241.

Mestas-Nuñez AM, Enfield DB. 1999. Rotated global modes of non-ENSO sea surface temperature variability. *Journal of Climate* **12**: 2734–2746.

Molinari RL, Mestas-Nuñez AM. 2003. North Atlantic decadal variability and the formation of tropical storms and hurricanes. *Journal of Geophysical Research* **30**: pp 48. DOI: 10.1029/2002GL016462.

Paz S, Tourre YM, Brolley J. 2008. Multitemporal climate variability over the Atlantic Ocean and Eurasia: linkages with Mediterranean and West African climate. *Atmospheric Science Letters* **9**: 196–201; DOI: 10.1002/asl.181.

Rajagopalan B, Kushnir Y, Tourre YM. 1998. Observed decadal midlatitudes and tropical Atlantic climate variability. *Geophysical Research Letters* **25**: 3967–3970.

Rayner NA, Parker DE, Horton EB, Folland CK, Alexander LV, Rowell DP, Kent EC, Kaplan A 2003. Global analyses of SST, sea ice and night marine air temperature since the late nineteenth century. *Journal of Geophysical Research* **108**: 4407. DOI: 10.1029/2002JD002670.

Rogel P, Tourre YM, Benoît V, Jarlan L. 2006. Tropical Atlantic moisture availability and precipitation over West Africa: application to DEMETER hindcasts. *Geophysical Research Letters* **33**: L21711. DOI: 10.1029/2006GL027178.

Schlesinger ME, Ramankutty N. 1994. An oscillation in the global climate system of period 65–70 years. *Nature* **367**: 723–726.

Tourre YM, White WB. 2006. Global climate signals and equatorial SST variability in the Indian, Pacific, and Atlantic oceans during the 20th century. *Geophysical Research Letters* **33**: L06716.

Tourre B., Rajagopalan Y, Kushnir Y, Barlow M, White W. 2001. Patterns of coherent decadal and interdecadal climate signals in the Pacific basin during the 20th century. *Geophysical Research Letters* **28**: 2069–2072.

Trenberth KE, Shea DJ. 2006. Atlantic hurricanes and natural variability 2 in 2005. *Geophysical Research Letters* **33**: L12704; DOI: 10.1029/2006GL026894.

Vecchi GA, Soden BJ. 2007. Increased tropical Atlantic wind shear in model projections of global warming. *Geophysical Research Letters* **34**: L08702. DOI: 10.1029/2006GL028905.

Vimont DJ, Kossin JP. 2007. The Atlantic Meridional Mode and hurricane activity. *Geophysical Research Letters* **34**: L07709. DOI: 10.1029/2007GL029683.

White WB, YM Tourre. 2007. A delayed action oscillator shared by the ENSO and QDO in the Indian Ocean. *Journal of Oceanography* **63**: 223–241. DOI: 10.1007/s10872-007-0024-7.

Zhang R, Delworth TL. 2006. Impact of Atlantic multidecadal oscillations on India/Sahel rainfall and Atlantic hurricanes. *Geophysical Research Letters* **33**: L17712; DOI: 10.1029/2006GL026267.

Zhang R. 2007. Anticorrelated multidecadal variations between surface and subsurface tropical North Atlantic. *Geophysical Research Letters* **34**: L12713. DOI: 10.1029/2007GL030225.

